Harmonic Klystron Frequency Converter

A. Leggieri, M. Behtouei, G. Burt, V. Dolgashev, F. Di Paolo, B. Spataro

***Abstract*— A new principle for the design of frequency converters, operating at significantly higher power and efficiency than previous devices, is described in this paper. The presented solution is implemented as a particular klystron topology for which a new design criteria is formulated through analytical expressions and a specific design procedure. The described frequency multiplier is suitable for telecommunications, non-lethal weapons or scientific and medical particle accelerators, where the most interested exploitation is in the field of high gradient particle acceleration and FEL devices for which no current sources meet the required performance. The frequency converter replaces all the low-level circuitry needed for frequency multiplication, representing a less expensive alternative. The presented structure can offer efficiencies in the range of 50-60% in the Ka-band with power levels of 20-30 MW without phase noise, sideband generation, jitter or chirp effects. The proposed principle is also applicable to other bands or power ranges.**

***Index Terms*— Klystrons, microwave amplifiers, microwave oscillators, frequency conversion, harmonic analysis.**

I. Introduction

As RF and mm-wave amplifiers move to higher frequencies it becomes harder to generate the required high driving powers as well as to measure, process and modify the drive signal to manage the output signal. In order to simplify the control loop, the signal is often down-converted to lower frequencies for manipulation before up-converting back to the operating frequency. Such circuitries, when implemented alongside electron tubes [1], [2], [3], [4], [5], [6] or solid-state devices [7], [8], [9] are affected by several limitations: image sidebands, phase noise, jitter and chirp. In addition to high efficiency amplification, by converting the intermediate frequency to the RF frequency, the proposed structure allows that such circuitry be removed. The klystron can be used as a frequency multiplier [10] and, recently, some upgraded solutions [11], [12] have been developed for that application; however they suffer from low efficiency (max 23%). We propose a comprehensive analysis of this mechanism and identify a solution to surpass these limitations. In the frame of the Compact Light XLS Project [13], a new design concept is proposed. Differently from klystron schemes such as BAC [1],COM [2], [3] and CSM [4], [5], harmonic cavities are used to produce convergent bunches and, differently from extended interaction klystrons [6], in the output structure the bunched beam excites two modes in the passband: one oscillation determines the output frequency (the "operating" mode) and a second one (the "auxiliary" mode) is superposed to create a condition to avoid reflected electrons, which is a typical challenge in the design of high efficiency klystrons. The latter oscillation is induced in the beam space charge by a dedicated harmonic gain resonator, which is installed before the output structure. A case study is reported to demonstrate the advantages of the proposed theory and design strategy. Without need of redesign or modification, by only adjusting the working point, the proposed frequency converter can operate above or below the traditional parameters for RF vacuum breakdown, hat are currently used as design criteria for normal conducting high gradient structures. This strategy allows the use of the same design to investigate different technologies and to identify their limits by only adjusting the working point (without redesign).

Manuscript received in DD MM AAAA; revised DD MM AAAA. Date of publication DD MM AAAA. The review was arranged by Editor XXXXXX.
Alberto Leggieri is with the Thales MIS, France; Franco Di Paolo is with the University of Rome Tor Vergata, Italy; Graeme Burt is with the Cockcroft Institute, UK; Valery Dolgashev is with the SLAC, Menlo Park, US; Mostafa Behtouei and Bruno Spataro are with National Institute of Nuclear Physics - National Laboratories of Frascati, Italy.

II. Limiting factors of the harmonic generation

It is well known that klystron efficiency decreases as the perveance increases [14] and that it scales with the harmonic order of the output (down to ~19% for a 3rd harmonic output). In this study, it has been observed that a major factor that limits the harmonic generation concerns the voltage V_{RF} applied to induce the modulation in the resonators. This effect is due to the harmonic current depth I_n, (that represents the portion of the DC current transferred to the nth harmonic) which, by varying the bunching parameter X, oscillates around a mean value making it impossible to maximise. By considering an electric space charge leaving the input cavity at the instant t_1, the modulated current arrives in the output cavity, after having traversed the distance l, at the instant t_2 defined in the phase space, as $\omega t_2 = \omega t_1 + \theta_0 - X\,sin(\omega t_1)$, where $X = M\,V_{RF}\,\theta_0/(2V_0)$ and M is the beam coupling factor which is the effective portion of the oscillating gap field experienced by the moving electron started with beam voltage V_0. The n^{th} harmonic of the modulated current can be expressed as an integral function of the oscillations at $n\omega t_2$ as well as a bilinear function of the single oscillation at ωt_1 [15],[16] as $|I_n(\omega t_1,\omega t_2)|/I_0 = |_0\int^{2\pi} e^{jn\omega t2}\, d\omega t_1 = 1/|1\text{-}Xcos(\omega t_1)|$. In the case of a small modulation depth, where $V_{RF} << V_0$, the oscillations in $|I_n|/I_0$ can be maximized between two maxima. However, when the shunt voltage V_{RF} at the input cavity reaches V_0, a portion of the modulated current is reflected from the output and only one of the two maxima persists for any X. Hence, the amplitude (that determines the full oscillation) of the harmonic current and the electronic efficiency are halved.

III. Proposed principle and synthesis method

In order to overcome the limitation described above, in addition to the use of a beam with a reasonably low perveance, the harmonic current oscillation is maintained at its peak value along the entire bunching circuit and reflected electrons are prevented in the output structure. A small modulation principle is adopted until the harmonic circuit, where the RF field is increased enough to effectively manage the harmonic response.

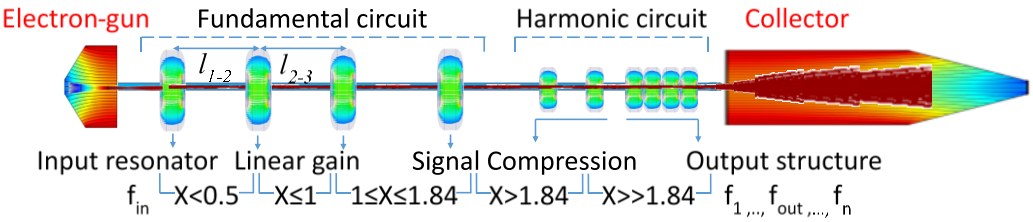

Fig. 1. Proposed frequency conversion structure: The fundamental circuit is composed by I) the input cavity, II) a set of low gain fundamental cavities and III) the fundamental signal compression stage. The harmonic circuit consists of I) the signal compression stage and II) the output structure.

In order to consider the space charge and non-linear effects, a hybrid design approach is proposed by means of semi-analytical design criteria within a large-signal computation.

A. Topology

For this aim, in the proposed multi cavity klystron (composed of N_{cav} resonators with individual RF gap voltages $V_{RF\,i}$= $V_{RF\,1\,,...,}V_{RF}N_{cav}$,) the desired condition on shunt voltages is obtained by making $V_{RF\,i}$ << V_0 until the last gain cavity (N_{cav}-1). The structure is arranged as represented in Fig.1.

The first part of the bunching sector is the "fundamental circuit" that consists of: I) the input cavity (resonating at f_{in}), II) a set of linear (low) gain fundamental cavities that operate between X<0.5 (to ensure sinusoidal bunching current) and X≤1 (because for X=1 the current becomes rich in harmonics [14]), and III) a fundamental signal compression stage that is composed by fundamental non-linear (moderate) gain cavities which operate with 1<X<1.84 (because, when X reaches the first root of the first derivative of the first kind Bessel function, n'_{11} = 1.84, the beam current grows exponentially [14]).

The second part is the "harmonic circuit" aimed to boost the space charge current. It consists of: IV) the signal compression bunching circuit which is composed of one or more harmonic gain resonators (whose last cavity oscillates at one specific Eigen-frequency of the output structure where X>1.84) and V) and the output structure which is implemented as a particular multiple cell resonator having X>>1.84.

Differently from the harmonic cavities commonly found in standard klystrons (which cause a reduction in beam core bunching due to divergent phases and a focusing of the anti-bunch), in the proposed configuration these cavities operate as gain resonators with convergent beam phase, resulting in continuous bunching where no sub-bunches are created. For this reason, the inductive tuning is used to adjust the frequencies of the harmonic gain resonators in order to be higher than the (harmonic) frequency desired for the output signal.

B. Gap voltages

Once the geometry of the cavities is sufficiently defined to broadly know the coupling factors M_i and the gap widths d_i; the gap voltages can then be established. By considering the output structure as a single cavity, the N_{cav} cavities of the klystron are numbered as: i=1 for the input cavity; from i=2 to i=N_{cav} -1 for the gain cavities and i=N_{cav} for the output. In order to reach the desired maximum electric field E_{max} in the output structure, while respecting the condition on the bunching parameters, an exponential configuration of the gap voltages V_{RFi} is proposed: For the i^{th} cavity, the gap voltage is defined by (1). Then, the external quality factors Q_{ext} for the input and output cavities are defined to get the desired gap voltages.

$$V_{RF\,i} = E_{Max}\, d_i\, e^{i-N_{cav}}. \quad (1)$$

C. Large-signal equivalent bunching parameters

For practical purpose and with limited physical signification, the concept of an equivalent bunching parameter for multiple drift spaces is proposed to assist the numerical design. It is assumed that the effect of the bunching between previous cavities is sufficiently low to be linearly added to the subsequent bunching effects without accounting for all permutations between drift spaces. In order to consider the space charge effects, the distances between cavity centers, l_i, are numerically defined with the aid of a large signal klystron interaction code: While observing the RF voltages calculated from the simulation, the cavity positions are adjusted until the gap voltages approach to the values V_{RFi} provided by (1) while the equivalent bunching parameters are calculated to verify that the conditions in section III. A) are respected at each iteration. By considering that the beam energy is distributed around eV_0 and the beam velocity around u_0, the large-signal equivalent bunching parameter between the cavities i-1 and i, is defined by

$$X_{i-1,i} = \sum_{h=2}^{i} M\ 2\pi f_{h-1} \frac{l_{h-1,h}}{u_0} \frac{V_{RF\,h-1}}{2\,V_0}. \quad (2)$$

D.Output structure

The efficiency and power output are enhanced by progressively increasing the current gain through the structure, culminating in a significant boost at the harmonic circuit to improve harmonic content. However, this increase can cause electrons to be reflected at the output. In order to prevent reflections, the output structure is implemented as a multi-cell resonator which contains at least one section that includes (within an opportune phase synchronism) a decelerating gap (to extract energy from the beam) and an accelerating gap (which can reaccelerate the possible reflected electrons). A coupled cavity system admits multiple normal modes; those whose frequencies are comprised in the space charge band (and exhibit a sufficient beam-coupling) are excited in the multi-cell system where they can overlap. The output structure is defined to exhibit, within a narrow frequency band (close to the output frequency), an initial section where two superimposed modes (an "operating" mode and an "auxiliary" mode) oscillate in phase opposition and a second section where the two modes oscillate in phase.

The first section ("constant current sector" in the right image of Fig. 2) forces the modulated beam current to remain constant and create a neutral zone for accelerations and decelerations while adding volume (to the rest of the output structure) where to distribute the RF power in order to reduce gap electric fields.

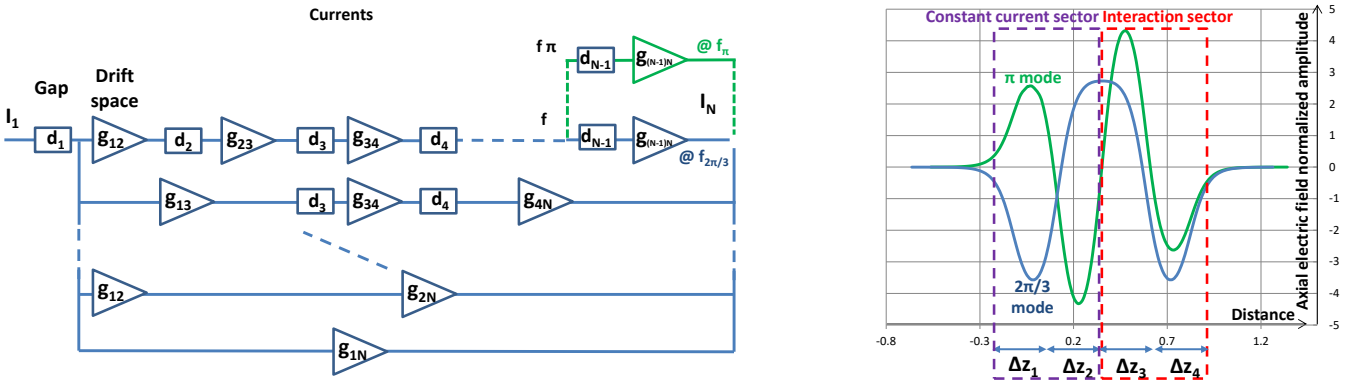

Fig. 2. On the left image, it is reported the feed-forward representation with the formalism in [14] in the small signal approximation that has been modified by adding in parallel the two last gain stages at the fundamental and output frequencies: the quantities d_i identify the cavity gaps and g_{ij} the gain. In the right image, the electric field mode patterns are reported: Δz_i are the widths (gap-to-gap spacing) of the output cells. The structure integrates a single harmonic gain cavity (resonating at $f_{space\ charge\ gain}$) and a four-coupled-cells output structure (whose two strong-interacting modes 2π/3 and π resonate at $f_\pi = f_{space\ charge\ gain}$ and $f_{2\pi/3} = f_{out}$ respectively).

The second section (identified as "Interaction sector" in the right image of Fig. 2), where the superposed modes are in phase, is used to extract the energy from the beam while mitigating electron reflections. The second section includes the output gap, where both modes exhibit decelerating fields, allowing for the possibility of reflections. Should an electron be reflected, it approaches in the previous gap where the two modes provide both accelerating fields. Once the supposed reflected electron approaches this gap, it is reaccelerated. This mechanism is limited by the phase conditions of reflected electrons, which shall arrive in the reaccelerating gap before the electric field commutates in the decelerating phase.

If the auxiliary frequency is higher than the output frequency (inductive tuning), the auxiliary mode contributes to the continued bunching process by contracting the space charge forces that are trying to elongate the bunch during the deceleration and by preventing fast de-bunching during the deceleration, resulting in an efficiency improvement. The output structure has a total interaction length $L'_{out}=\lambda_e=u_0/f_{out}$ that is longer than the beam wavelength at the desired multiplied frequency f_{out}. This condition can be achieved if the gap-to-gap spacing Δz and the gap width d of the coupled cells of the output structure are equal, thus $\Delta z'=d'_{output}=L'_{out}/N_{cell}= u_0/(f_{out}/N_{cell})$.

If the beam voltage is strong enough to allow the electron to cross a gap length equal in a free-space $\lambda/4$ of the third harmonic, while not exceeding half period, mixed accelerations-decelerations are prevented.

Then, if high beam voltages are used where $u_0/c>½$ (convenient for a high efficiency multiplier), the interaction region length is chosen as a quarter wavelength of the RF output frequency. Since it is not possible to create a gap longer than the gap-to-gap spacing inside a multi-cell oscillator, the gap-to-gap spacing is at most equal to the gap width: $\Delta z = d_{out} = L_{out}/N_{cell}= c/(f_{out}/N_{cell})$. An equal number of cavities is assigned to the two sections. Being N_{harm} the harmonic order of the desired output signal, the output frequency of the converter is $f_{out}=N_{harm} f_{in}$ and the gap widths d of the output cells are By choosing $N_{cell} = 4$, the gap-to-gap distance and the gap width should match the quarter wavelength of the output frequency $\Delta z=d_{out} =\lambda_{out}/4$. In this case, four modes resonate in the output structure: 0, π/3, 2π/3 and π mode.

$$d = \begin{cases} \dfrac{u_0/c}{N_{harm}}\dfrac{\lambda}{N_{Cell}} & if \dfrac{u_0}{c} \le ½\,, \\ \dfrac{1}{N_{harm}}\dfrac{\lambda}{N_{Cell}} & if\ 1 > \dfrac{u_0}{c} > ½\,. \end{cases} \tag{3}$$

The 2π/3 mode and the π mode are the two desired modes to be superposed (as shown in Fig.2). The frequency of the 2π/3 mode (operating mode) determines the output frequency of the structure ($f_{2\pi/3} = f_{out} = N_{harm} f_{in}$) and that of the π mode (auxiliary mode) determines the space charge harmonic component that is submitted to the high gain ($f_\pi = f_{space\ charge\ gain}$).

As the effective impedance of the mode is proportional to M^2, in order to ensure significant excitation, the two desired modes should exhibit a relatively high beam-coupling factor $M\ge0.6$. The other (unwanted) modes present in the passband (0 and π/3, whose excitation is undesired) should have a reasonably lower coupling with the beam (the authors suggest that ⅓ of the beam coupling of the desired modes is a good compromise): $M\le 0.2$. This final condition on the unwanted modes is essential for the first section of the output structure, while it is less critical for the second section. In the latter, as the beam velocity varies considerably throughout the system, the unwanted modes exhibit significant frequency detuning (lower frequencies) compared to the frequency and harmonics of the bunches, thus restricting their influence on the wave-to-beam interaction.

The resonant frequency of the unperturbed cell f_0 and the cell-to-cell coupling factor k are established to make the 2π/3 Eigen-solution of the coupled oscillator [17] equal to the desired output frequency f_{out} with the condition to have the same field components at the two extremities (that is required to consider the effect of drift tubes) as defined by the (4).

$$f_q = \frac{f_0}{\sqrt{1+k\cos\left[\frac{q\,\pi}{N_{Cell}-1}\right]}}; \qquad \alpha = q\frac{\pi}{N_{Cell}-1}\,,\ q = 0,\ 1,\ 2, \ldots,\ N_{Cell}-1. \tag{4}$$

Where α is the mode order that gives the phase shift between adjacent cells and k=2[Max{f_q}-Min{f_q}]/ [Max{f_q}+Min{f_q}] individuates the field ratio and the frequency detuning.

E. Harmonic gain resonators

One or more dedicated harmonic gain resonators are installed before the output coupler in order to induce the oscillation at the frequency of the π mode in the space charge current. Since this frequency component ($f_\pi = f_{space\ charge\ gain}$, that once injected in the output structure excites the π mode) is higher than the harmonic ($f_{out}=N_{harm}\ f_{in}$) of the bunch frequency (f_{in}), the inductive tuning of the harmonic resonators produces convergent phase bunching. It was later found in simulation that the deviation from this requirement resulted in a lower efficiency, being the inductive tuning an usual method for improving beam wave interaction.

F. Global parameters and harmonic analysis

Due to the dependence on large signal effects [14], [16], a numerical design procedure is required.

I) A predefinition, based on the proposed criteria (in sections III.B and III.C), is used to determine the distances between cavities $l_{i-1,i}$, the beam coupling factors M_i and the R_i/Q_i, in order to approach to the desired gap voltages $V_{RF\,i}$ while respecting the constraints on the bunching factors $X_{i-1,i}$.

II) A numerical optimization is performed to make the desired harmonic current have the same modulation depth of the fundamental $I_n = I_1$ while verifying that the conditions on the bunching parameters $X_{i-1,i}$ are still respected by adjusting the resonant frequencies of the fundamental cavities as well as the Q_{ext} of the input cavity and the position of the harmonic circuit. Since the boost of the space charge, aimed to increase the harmonic content, causes the fundamental component to expand (over bunch) while traversing the harmonic circuit, the adjustment of these parameters optimizes the modulated depths and coupling factors, aiding the bunch lengths of both the fundamental and the desired harmonic to reach similar values when they pass through the output gap and increases the power.

A series of harmonic current packages is produced in the output structure: Being I the amplitude of the total current, when the efficiency is maximized, the time domain modulation depths of harmonic current in the output section follow the (5).

$$I(t) = I\sum_{n=1}^{N_{harm}} sin(n\omega t + \varphi_n) + I\sum_{p=1}^{\infty}\frac{\pi}{N_{harm}+p}\sum_{n=pN_{harm}+1}^{N_{harm}(p+1)} sin(n\omega t + \varphi_n)\,. \qquad (5)$$

G. Cavity profiles

The numerical modelling is simplified by excluding overmoded cavities. For this reason, in the analysed structure, all resonators operates in the TM_{010} fundamental mode and higher order modes are assumed to not be excited. Since the harmonic cavities are aimed to provide gain at the harmonic frequency, their diameters are chosen to make them resonate close (depending on the tuning) to a multiple of the input frequency. If only fundamental resonators are considered for the modelling, Pillbox shapes can be favoured for harmonic cavities due to their simpler profile (without nose-cones), which in practice can also ease manufacturing of smaller resonators that are required to operate at higher frequencies (harmonic) than those close to the fundamental frequency. Re-entrant shapes are indicated for input cavity and linear gain oscillators because, respect to Pillbox, they typically provide higher R/Q even having complex shapes that remain reasonably simple to be machined for lower frequencies (close to the fundamental).

The effect of the beam stratification caused by both the radial variation in the space charge forces and the radial variation of the gap voltages, can be exploited to create a sufficient bunching for the inner part of the beam in order to increase the harmonic content [3], [18]. In the absence of nosecones, Pillbox cavities show a moderate enhancement of the electric field in the innermost radial region [19] if compared to Re-entrant cavities, where stronger fields are concentrated at the edges of the nose cones [17]. The tendency to exhibit uniform fields over the bunch and the over focusing of the beam edge suggests that Pillbox shapes can be beneficial for the harmonic circuit.

The beam (drift tube) tunnel is defined to put under cut off all the frequencies considered in the structure (by verifying that its radius provides a TE_{11} cut off frequency higher than that of the TM_{010} modes of the cavities) [13], excluding the transmissions between cavities (except for those composing the output structure where the multi cell interaction is desired).

The modelling of higher-order modes in harmonic cavities and the harmonic transmission in the beam tunnel is planned to analyse the effects on beam coupling, output power enhancement and mitigation of electron reflections. Being out of the scope of this paper, this study is not reported here.

IV. Application to Ka-band: Simulations and Results

The structure has been developed by adopting the electron beam defined in [13] whose main features are: V_0=480 kV, I_0= 100 A and a radius r_b=1 mm. The beam tunnel, with r_a=1.2 mm radius, exhibits a fundamental mode cutoff at f_a = 73 GHz that ensures all TM_{010} cavity frequencies are under cut off. The bunching circuit is composed by 5 cavities and the output structure by 4 cells, giving N_{cav} = 6. The design has been performed with the large signal code KlyC [20] that has been previously validated by several tests and measurements as well as crosschecked with other commercial and industry-reserved codes, including CST, MAGIC and Thales Klys-2D [20].

The structure has been preliminarily defined following the indications in point I) of section III.F: By imposing a maximum electric field E_{max}=250 MV/m, the (1) gives $V_{RF\,1}$ = 3.5 kV for the input (reentrant) cavity, obtained with Q_{ext} = 27 for P_{in}=500W. By placing the first gain (reentrant) cavity at $l_{1,2}$ =56 mm from the input, the desired value $V_{RF\,2}$ = 9.5 kV has been obtained (with an inductive tuning at f_2=12.14 GHz) so that the drift space exhibits an equivalent bunching parameter $X_{1,2}$ = 0.06 calculated by (2) that respects the requirement in section III.A. The rest of the structure has been preliminary defined with the same approach. One harmonic resonator (pillbox cavity), aimed to induce the f_π phasor, has been placed at $l_{5\text{-}6}$ = 19 mm before the output structure; which is composed by 4 (pillbox) cavities defined with the (3) and (4) and (having $\Delta z = d = 2.08$ mm) operates in the 2π/3 mode at $f_{2\pi/3}$ = 36.00 GHz. With the given profile, the output structure exhibits a π mode frequency f_π = 36.61 GHz. The single-cell unperturbed frequency is 35.50 GHz and $k = 0.055$ determines a drift tube radius r_a = 1.2 mm for the cell electric coupling.

After this predefinition step, the structure has been numerically adjusted following instructions in point II) of section III.F, providing the values in the left table of Fig. 3.

f0(MHz)	R/Q (Ω)	M	Qe	Qin	z (mm)
12000	112.4988	0.9295	52	5.4269e+03	0
12085	112.9896	0.9289	100000	5.4267e+03	56
12280	116.4531	0.9248	100000	5.4350e+03	102
12547	116.4531	0.9248	100000	5.4350e+03	197
3.6615e+04	108.2822	0.6832	100000	3.8807e+03	274
3.5478e+04	109.4702	0.6928	100000	3.8329e+03	293
3.5478e+04	109.4702	0.6928	100000	3.8329e+03	295.3400
3.5478e+04	109.4702	0.6928	100000	3.8329e+03	297.6800
3.5478e+04	109.4702	0.6928	14.5000	3.8329e+03	300.0200

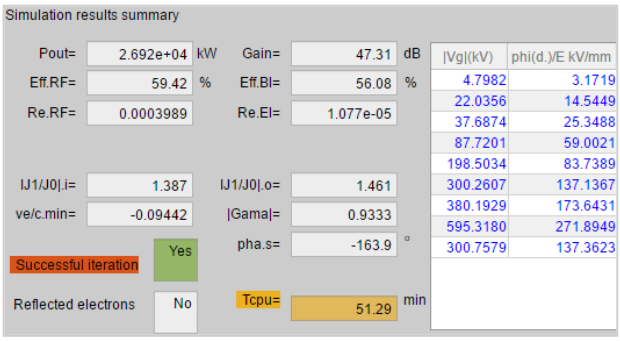

Fig. 3. KlyC software set-up interface describing electrical parameters and gap center positions for each cavity (left) and simulation output (right).

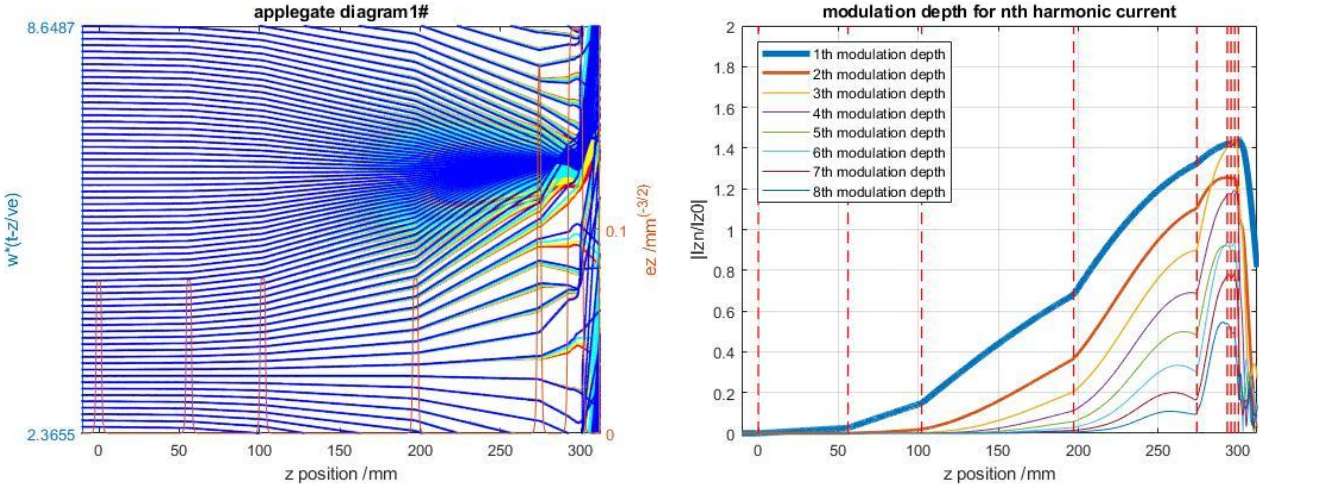

Fig. 4. Applegate diagram with cavity fields (left) and modulation harmonic currents (right) where the harmonic packages identified by (5) are visible.

In the left image of Fig. 4, the Applegate diagram shows an over bunching before the output gap which provides sufficient bunching for the inner part of the beam to obtain a high harmonic content; while the outer part is over bunched and starts expanding again (hence reducing its harmonic content from a very high peak) with the output gap placed when the both have equal bunch length and similar harmonic currents.

In the right image of Fig. 4, the possible (normalized) currents (obtained from the same set of cavity parameters [20]) at different harmonics are shown. Since KlyC computes the power for the frequency at which the RF field oscillates [20], the yellow curve (3rd harmonic) shall be considered for the output structure and the last gain cavity while the blue curve (1st harmonic) refers to other cavities.

The harmonic packages, described by the (5), are reported in Table I and Table II in terms of current harmonic ratios (I_n/I_o) and expected single power outputs P_{out} for different frequencies of the output structure (in whose bands the RF voltages are excited and no power is provided to other harmonics).

The harmonic ratios are obtained by normalizing the values (given by KlyC simulation and visible in the right image of Fig. 4) of the harmonic currents (I_n) to the value of the actual output harmonic (I_o). For the estimation of new possible power outputs at different harmonics, it is assumed that the output structure is replaced by a new resonator designed to oscillate in the $2\pi/3$ mode at the new output harmonic with the same gap voltages of the actual structure. Since no voltage is not applied to the harmonics whose frequencies are out of the cavity bands [20], the new possible power outputs are estimated by multiplying the harmonic ratios (in Table I) to the value of the actual power output (26.9 MW). The higher frequency achievable is given by the TE_{11} mode cutoff of the beam tunnel, which limits the upgradeability of the case study structure to the 6th harmonic because, for higher frequencies, the beam tunnel does no longer cut off the generated signals and cavities unwantedly couple.

The equivalent bunching parameters are reported in Table III. These values are calculated with the (2) by using the RF fields issued from the large signal computation at the harmonics at which the cavities operate. An electronic efficiency of 56.1% and a gain of 47.3 dB with ~3% of Ohmic losses have been obtained alongside an output power of 26.92 MW at the 3rd harmonic of the drive frequency at the input. The minimum electron velocity -0.095·c respects the requirement v_{min}>-0.1c. No reflected electrons nor monotron oscillations are detected. The absence of coupling between the harmonic oscillator (last gain cavity) and the output structure is visible in the left image of Fig.3 where the electric field (red line) falls to zero.

TABLE I
HARMONIC CURRENT RATIOS: I_N/I_O

Order N_{Harm}	Ratio I_n/I_o	Order N_{Harm}	Ratio I_n/I_o	Order N_{Harm}	Ratio I_n/I_o
1st	1.00	4th	0.83	7th	0.55
2nd	0.88	5th	0.65	8th	0.38
3rd	1.00	6th	0.65	9th	0.35
Ideal 1-2-3	1.00	Ideal 4-5-6	$\pi/4$=0.78	Ideal 7-8-9	$\pi/5$ = 0.63

TABLE II
EXPECTED POWER OUTPUTS: P_{OUT} [MW]

Order N_{Harm}	P_{out} [MW]	Order N_{Harm}	P_{out} [MW]	Order N_{Harm}	P_{out} [MW]
1st	26.9	4th	22.4	7th	14.7
2nd	23.7	5th	17.5	8th	10.4
3rd	26.9	6th	17.5	9th	9.4
Ideal 1-2-3	26.9	Ideal 4-5-6	21.0	Ideal 7-8-9	17.0

TABLE III
LARGE-SIGNAL EQUIVALENT BUNCHING PARAMETERS *X*

Drift space	1-2	2-3	3-4	4-5	5-6
X parameter	0.08	0.39	1.49	3.55	7.01
Requirement	<0.5	≤1	1< *X* <1.84	>1.84	>>1.84

The -3dB bandwidth [14] is BW=60 MHz (0.5%): It determines a minimum pulse length of 16.6 ns that complies with 1.5 μs requirement of the Compact Light XLS project [13].

With the intrinsic low perveance, the proposed design could be implemented as a multibeam klystron [21] to increase power and efficiency. In that case, the exploitation of higher order modes is crucial to enhance the performance of the structure.

The max gap voltage (595.3 kV) is produced when $2\pi/3$ and the π mode harmonics enter with the same phase in the 3rd cell of the output structure, determining the max electric field (271.9 MV/m that exceeds the desired value by ~ 9%). It is remarked that this field can be reduced by detuning the individual frequencies of the cells or by using larger apertures (the reduction of the total impedance can be compensated by increasing the number cells). The efficiency of the described frequency converter can be improved by replacing the last two gain cavities of the fundamental circuit with a BAC cavity triplet [1] (containing a harmonic cavity whose harmonic index is $1<N<N_{Harm}$) by following the procedure in [22]. In accordance with this strategy, by using a 2nd harmonic cavity, the electron efficiency has been shown in simulation to increase from the 56% to 62% and the power from 26.92 MW to 29.85 MW. The maximum electric field (in the penultimate output cell) has been increased from 274.4 kV to 295.6 kV. Being out of the scope of this paper, this step is not described here.

V. TECHNOLOGICAL FEASIBILITY ANALYSIS

In order to assess the feasibility of the case study device, the cold measurements and the main parameters for vacuum RF breakdown on similar cavities have been analyzed. The X band cavities, used in the simulated structure, have the same profile of the resonators integrated in the SPARC linearizer, which are manufactured by standard milling [23], [24]. The Ka band cavities have the same profile of the single–feed mode launcher resonators of the CLIC accelerator [25], [26], which are manufactured with high speed milling using diamond tools and intermediate stress relieve heat treatments [27]. The second aspect that has been analyzed is the compliance with the main parameters for vacuum RF breakdown prediction on high gradient structures. The Eigen-solutions of cavity fields have been normalized to the KlyC [20] large signal output in order to calculate the maximum surface electric fields $|E|_{\max}$ and modified Poynting vectors S_c as well as the surface pulsed temperature increase ΔT, by following the indications in [23]. The resulting $|E|_{\max}$ considers the effects of gap field on real cavities. The highest fields are located in the gaps 6 to 9, which are present in pillbox cavities (where the absence of nose cones confers a reduced field enhancement with respect to reentrant shapes). The highest gap field (271.9 MV/m reported in Fig. 3, right image, last column) corresponds to a surface electric field of 276.1 MV/m (Table IV, line 9, column $|E|_{\max}$) that exceeds by ~10% the 250 MV/m breakdown criterion [28], meaning that the structure operate above the traditional parameters for RF vacuum breakdown. In order to ensure that all criteria are respected without redesigning the structure, the operating point has hence been lowered. As shown in Table V, a "safe" working point (with a beam voltage V_b=455.21 kV and a beam current I_b=94.84 A) allows to achieve P_{out}=22.27 MW and η = 51.6 % while ensuring $|E|_{\max}$= 249.3 MV/m and S_c = 4.6 W/μm^2. This figure ensures that cavity sizes have sufficient power capacity to avoid ignition and breakdown, especially for harmonic resonators (described in Table V, lines 5 to 9).

TABLE IV
BREAKDOWN PREDICTION AT CRITICAL WORKING POINT
V_B=480 kV, I_B=100 A, P_{IN} = 500 W, P_{OUT} = 26.92 MW, η = 56.1 %

Cavity	$\|E\|_{\max \text{ surface}}$ [MV/m]	ΔT [°C]	Sc [W/μm^2]
1	3.2	0.0	0.0
2	14.7	0.0	0.0
3	25.6	0.0	0.0
4	59.3	1.6	0.3
5	84.1	1.1	0.4
6	139.0	10.8	1.7
7	176.4	11.5	2.3
8	276.1	28.2	5.6
9	139.5	7.2	1.4
Criteria	< 250	< 50	< 5

TABLE V
BREAKDOWN PREDICTION AT SAFE WORKING POINT
V_B=455.21 kV, I_B=94.84 A, P_{IN} = 500 W, P_{OUT} = 22.27 MW, η = 51.6 %

Cavity	$\|E\|_{\max \text{ surface}}$ [MV/m]	ΔT [°C]	Sc [W/μm^2]
1	3.2	0.0	0.0
2	15.4	0.0	0.0
3	27.6	0.0	0.0
4	-63.9	1.9	0.4
5	82.6	1.1	0.4
6	-215.0	25.8	4.2
7	160.3	9.5	1.9
8	249.3	22.9	4.6
9	126.7	5.9	1.2
Criteria	< 250	< 50	< 5

As recently reported [29], [30], [31] multiple cavities of similar dimensions (manufactured with traditional techniques) have shown full compliance with the main parameters for vacuum RF breakdown on high gradient structures. Since the proposed device should operate at the critical working point, once the mockup is manufactured, one can investigate the breakdown limits by increasing the current and beam voltage at constant perveance. By considering that the case study structure is designed for a pulse duration of 1.5 μs [13], a short pulse mock-up can be a suitable solution at a reasonable cost for investigational activity. The KlyC [20] code has been validated for a klystron-based frequency converter by simulating in the CST PIC solver a 3-cavities sample structure with f_{in}=35 GHz, f_{out}=105 GHz, P_{in}=10 W, V_0=30 kV, I_0=200 mA and r_b=0.2 mm [11]: Consistent results were provided, for instance $V_{RF3\ CST}$=0.750 kV and $V_{RF3\ KlyC}$=0.744 kV for output gap voltages.

Being out of the scope of this paper, this analysis is not described here; however, several other benchmarks of KlyC are available in literature for Klystrons [11], [12], [20], [21]. PIC simulations aimed at verification of the possibility of reflected electrons in the collector, the beam stratification in real cavity fields and beam scalloping are planned for the next step of this research. The presented results give significant confidence in the proposed topology and methodology and provides a solid basis for future high power frequency converters.

VI. Conclusion

A novel design methodology for the implementation of frequency converters in the form of klystron amplifiers is proposed. The device is defined by a special topological arrangement and a specific procedure that relies on new design criteria formalized through analytical expressions that assist the numerical definition of the interaction structure.

The proposed design approach has been verified by the modeling of a case study device dedicated to the Compact Light XLS project, which is aimed to provide a 36 GHz output with a 12 GHz input. The simulations show an electronic efficiency of η = 56.1 % and a 3rd harmonic power P_{out} = 26.9 MW. Without need of physical modifications and by only adjusting the working point, the structure can operate with electronic efficiencies higher than 50% at different power levels (ranging from 22 MW to 27 MW), below or above the traditional thresholds of vacuum breakdown parameters for high gradient structures, giving the possibility to investigate the limits of new technologies. By replacing the last two gain cavities with a BAC triplet (including a 2nd harmonic cavity) the electron efficiency increases to the 62% providing 29.85 MW of power output at the 3rd harmonic of the drive frequency. The proposed design criteria and procedure are applicable to other bands or power levels: A 4 GHz input can be used for 8 GHz or 12 GHz output as well as for 16 GHz or 20 GHz, by exploiting the 2nd or 3rd as well as the 4th or 5th harmonic respectively.

References

[1] I. A. Guzilov, “BAC method of increasing the efficiency in klystrons”, 2014 Tenth International Vacuum Electron Sources Conference (IVESC), 30 June-4 July 2014.

[2] A. Baikov, C. Marrelli, and I. Syratchev, ‘Toward High Power Klystrons with RF Power Conversion Efficiency on the Order of 90%.’IEEE Transactions on Electron Devices, Vol. 62, No. 10, October 2015.

[3] D. A. Constable et Al., “High Efficiency Klystron Development for Particle Accelerators”, Proceedings of eeFACT 2016, Daresbury, UK.

[4] C. Marrelli, ‘Towards more efficient klystron designs’, TIARA Workshop on RF Power Generation for Accelerators, 17 - 19 Jun 2013, Uppsala, Sweden.

[5] X. Chang, Y. Jiang, S. V. Shchelkunov, and J. L. Hirshfield, “Ka-Band High Power Harmonic Amplifier for Bunch Phase-Space Linearization”, presented at the North American Particle Accelerator Conf. (NAPAC'19), Lansing, MI, USA, Sep. 2019, paper WEPLM51.

[6] H. Zhang, D. Zhao, J. Luo, "The beam-wave interaction calculation of a Ka-band Extended Interaction Klystron", IEEE International Vacuum Electronics Conference (IVEC), Monterey, USA ,19-21 April 2016.

[7] Leggieri, A., Orengo, G., Passi, D., Di Paolo, F., “The Squarax spatial power combiner”, Progress In Electromagnetics Research C, 2013, 45, pp. 43–55.

[8] Leggieri, A., Passi, D., Saggio, G., Di Paolo, F.,”Multiphysics design of a spatial combiner predisposed for thermo-mechanically affected operation”, JEMWA, 2014, 28 (17), pp. 2153–2168.

[9] A. Leggieri, D. Passi, F. Di Paolo, G. Saggio, “Global Design of a Waveguide X-Band Power Amplifier”, International Journal of Simulation, Systems, Science and Technology, Vol. 15, Issue 4, Aug. 2014, pp. 57-69.

[10] V. J. Norris, "The frequency-multiplier klystron", Int. J. Electron., vol. 1, no. 5, pp. 477-486, 1956.

[11] G. Burt, L. Zhang, D. A. Constable, H. Yin, C. J. Lingwood, W. He, C. Paoloni, A. W. Cross, "A Millimeter-Wave Klystron Upconverter With a Higher Order Mode Output Cavity," in IEEE Transactions on Electron Devices, vol. 64, no. 9, pp. 3857-3862, Sept. 2017.

[12] S. M. Razavi, E. Hamidi and S. M. J. Razavi, "A 10-kW Output Power Ka- to W-Band Klystron Harmonic Generator," in IEEE Transactions on Electron Devices, vol. 70, no. 6, pp. 2852-2859, June 2023.

[13] Bruno Spataro, Mostafa Behtouei, Franco Di Paolo, Alberto Leggieri, “A low-perveance electron gun for a high-efficiency Ka-band klystron” The European Physical Journal Plus, Vol 137, Number 769. 2022.

[14] G. Caryotakis, High Power Klystrons: Theory and Practice at the Stanford Linear Accelerator Center SLAC-PUB 10620, 2005, pp.34-35.

[15] R.Warnecke and P. Guénard, “Multiplicateurs de fréquences” in “ Tubes Électroniques à Commande par Modulation de Vitesse” Gauthier-Villars, Paris, 1951.

[16] S.E. Tsimring, Electron Beams and Microwave Vacuum Electronics, Wiley, 2007; pp. 267.

[17] A. Leggieri, D. Passi, F. Di Paolo, A. Ciccotelli, S. De Stefano, F. Marangoni, G. Felici, "Real-Time Beam Monitor for Charged Particle Medical Accelerators", IEEE Transactions on Nuclear Science, Volume: 63, Issue: 2, April 2016, pp: 869 - 877.

[18] D. A. Constable, C. Lingwood, G. Burt, A. Y. Baikov, I. Syratchev and R. Kowalcyzk, "MAGIC2-D Simulations of High Efficiency Klystrons Using the Core Oscillation Method," *2017 Eighteenth International Vacuum Electronics Conference (IVEC)*, London, UK, 2017, pp. 1-2.

[19] A.V. Smirnov, J. Zeng, "Analytical Characterization of Fundamental Mode in Pillbox Cavities with Beam Pipe", Nuclear Instruments and Methods in Physics Research Section A, Volume 452, Issues 1–2, 2000, pp. 44-52.

[20] J. Cai, I. Igor Syratchev, "KlyC: 1.5-D Large-Signal Simulation Code for Klystrons”, IEEE Transactions on Plasma Science, Volume 47, Issue 4, April 2019, pp. 1734 - 1741.

[21] J. Cai, I. Igor Syratchev, "Modeling and Technical Design Study of Two-Stage Multibeam Klystron for CLIC", IEEE Transactions on Electron Devices, Volume 67, Issue 8, Aug. 2020, pp. 3362 – 3368.

[22] A. Jensen, A. Haase, E. Jongewaard, M. Kemp, J. Neilson, "Increasing Klystron Efficiency Using COM and BAC Tuning and Application to the 5045 Klystron", 17th IEEE International Vacuum Electronics Conference 19-21 April 2016. Monterey, CA, US.

[23] D. Alesini et al, “Design and RF measurements of an X-band accelerating structure for linearizing the longitudinal emittance at SPARC”, Nuclear Instruments and Methods in Physics Research A 554 (2005), pp. 1–12.

[24] A.Falone, “Sviluppo e Test di una Cavità Accelerante Multi-Cella ad 11.4GHz”, Master Degree Thesis in Electronic Engineering, Academic year 2003-2004, University of Rome “Sapienza”, 2004.

[25] L. Sanchez, F. Aragon, J. Calero, D. Carrillo, D. Gavela, J. L. Gutierrez, A. Lara, E. Rodriguez, F. Toral, S. Doebert, G. Riddone, A. Samoshkin, “Work on PETS Developed at CIEMAT”, Int. Workshop on Future Linear Colliders (LCWS) 2011, 26-30 September 2011. Granada, Spain.

[26] I. Syratchev, “Mode Launcher as an Alternative Approach to the Cavity-Based RF Coupler of Periodic Structures”, PS/RF/ Note 2002-013, CLIC Note 503, Geneve, 2002.

[27] S.Doebert, Y. Raguin, I. Syratchev, W. Wuensch “Coupler Studies for CLIC Accelerating Structures” Proceedings of EPAC 2002, Paris, FR.

[28] M. Diomede, “Main parameters for vacuum RF breakdown prediction” in “High-gradient structures and RF systems for high-brightness electron LINACS”, doctoral Thesis, Università Sapienza Roma, Feb. 18, 2020.

[29] V.Dolgashev, Sami Tantawi, Yasuo Higashi, Bruno Spataro, “Geometric dependence of radio-frequency breakdown in normal conducting accelerating structures”, Appl. Phys. Lett. 97, 171501 (2010).

[30] B. Spataro, D. Alesini, V. Chimenti, V. Dolgashev, Y. Higashi, M. Migliorati, A. Mostacci, R. Parodi, S.G. Tantawi, A.D. Yeremian, "High power comparison among brazed, clamped and electroformed X-band cavities", NIM-A-657 (2011) 88-93.

[31] V. A. Dolgashev, L. Faillace, B. Spataro, S. Tantawi, R. Bonifazi, “High Gradient RF tests of Welded X-Band Accelerating Structure”, Physical Review Accelerators and Beams 24, 081002 (2021).